Effects of Peripheral Substituents and Axial Ligands on the Electronic Structure and Properties of Cobalt Porphyrins

Meng-Sheng Liao, John D. Watts, and Ming-Ju Huang*

Department of Chemistry, P.O. Box 17910, Jackson State University, Jackson, Mississippi 39217

Received: July 25, 2005

The effects of peripheral substituents and axial ligands (L) on the electronic structure and properties of cobalt tetraphenylporphyrin (CoTPP) have been studied using DFT methods. Various density functionals were tested, and the ground state of each system was determined by considering several possible low-lying states. The ground states of the fully fluorinated $CoTPPF_{28}(L)_2$ complexes with L = THF, Py, and Im were identified to be high-spin (^4E_g) by the meta-GGA functional τ-HCTH, which contains the kinetic energy density τ, in agreement with experimental measurements. All the pure GGA functionals, including the recently developed mPBE, OPBE, and HCTH/407, show more or less overestimation of the relative energies of the high-spin states. The energy gap between the $^2A_{1g}$ and ^4E_g states is insignificant (~0.1 eV) and varies in the order L = Py < L = THF < L = Im. The results and their trend are consistent with ^{19}F NMR studies which show partial population of the ^4E_g state in $CoTPPF_{28}(THF)_2$ and $CoTPPF_{28}(Py)_2$ and a complete conversion to the high-spin state in $CoTPPF_{28}(1\text{-MeIm})_2$. Upon coordination by two very strong field axial CO ligands, $CoTPPF_{28}(CO)_2$ becomes low-spin, as in unligated $CoTPPF_x$. The influence of the peripheral substituents and axial ligands on the ionization potentials, electron affinities, and $CoTPPF_x-(L)_2$ binding strength was also investigated in detail.

1. Introduction

Metal porphyrins (MPors), with their square planar structure, are very interesting compounds that continue to be the subject of intense research. (Here, we use Por to refer to any porphyrin.) In addition to the well-known models for metalloproteins and enzymes in biology, MPors have also found a variety of applications in different fields that include coordination chemistry and catalysis, as well as materials science.[1] Metal tetraphenylporphyrin (MTPP) and metal octaethylporphyrin (MOEP) are the two most popular synthetic metal porphyrins. MPors show a wide range of chemical and physical behaviors, depending on the nature of the macrocycle, the central metal, and the axial ligands (if any). On the other hand, it has been shown that the properties of MPors can be effectively modulated with different substituents in the periphery of the macrocycle. For example, the introduction of eight halogen atoms in the pyrrole rings in TPP produced large spectral and oxidation potential shifts.[2] Some halogenated MTPPs are also much more active as catalysts than pure MTPPs, and both the stability and the activity of the catalysts increase with the extent of halogenation.[3] There has been a great deal of interest in substituent effects in porphyrins. Recently, two research groups[4−6] reported the synthesis and characterization of metal octafluoro-tetrakis(pentafluorophenyl)porphyrins, $MTPPF_{28}$ (see Figure 1), where all the H-atoms in MTPP at the β-pyrrole and *meso*-phenyl positions were replaced by F-atoms. $MTPPF_{28}$ represents the most electron-deficient metal porphyrin among the $MTPPF_x$ species and is demonstrated to be an extremely oxidatively robust material.[6] Among the various metals M, $CoTPPF_{28}$ is of particular interest. The X-ray crystal structure measurements by DiMagno et al.[5] on $CoTPPF_{28}$ in the presence of two tetrahydrofuran (THF = OC_4H_8) axial ligands show a large porphyrin core expansion of 0.08 Å as compared to $CoTPPF_{28}(toluene)_2$, indicating the occupation of the Co $3d_{x^2-y^2}$ orbital in the six-coordinate $CoTPPF_{28}(THF)_2$ complex, which results in increased repulsion between the metal and the porphyrin nitrogens. According to DiMagno et al.,[5] $CoTPPF_{28}$ is the first example of a porphyrin that supports a high-spin cobalt ion.

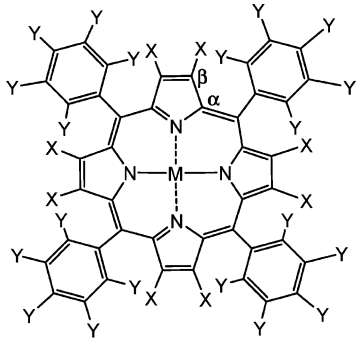

Figure 1. Molecular structure of metal tetraphenylporphyrins (MTPPs) and their fluorosubstituted derivatives.

It is well-known that iron^{II} porphyrins can exist as low-spin ($S = 0$), intermediate-spin ($S = 3/2$), and high-spin ($S = 2$) states, depending on the coordination and environment of the iron ion.[7] In contrast, the electronic state for cobalt^{II} porphyrins is generally low-spin $^2A_{1g}$ and is insensitive to the environment (mainly the type and number of axial ligands) around Co^{II}. The difficult spin-state transition in Co^{II} is attributed to a relatively

* Corresponding author. Email: mhuang@chem.jsums.edu.

10.1021/jp058212b CCC: $30.25 © 2005 American Chemical Society
Published on Web 12/01/2005

small electron exchange energy in high-spin ($S = {}^3/_2$) Co^{II} as compared to that in high-spin Fe^{II}.[5]

Polyhalogenated porphyrins have also been the subject of some theoretical studies. Pachter et al.[8] performed density functional theory (DFT) calculations on a series of $ZnTPPX_8$ molecules with X = F, Cl, and Br, aimed at accounting for the effects of the halogen substituents on the spectral shifts. In the early 1990s, Ghosh et al.[9] carried out Hartree−Fock (HF) and DFT calculations on a series of free-base H_2TPPF_x ($x = 0$, 8, 20, 28) molecules, mainly devoted to ionization potentials. So far, little is known about the effects of peripheral substitution on the electronic structure (mainly electronic state) of metal porphyrins.

In this work, we present a theoretical investigation on the electronic structure of a series of $CoTPPF_x(L)_2$ complexes with $x = 0$, 8, 20, and 28 and L = THF, pyridine (Py), Imidazole (Im), and CO. Here, THF is a pure σ-donor and can bind a metal only weakly. The nitrogenous bases Py and Im have strong σ-donor capacity but are relatively weak π-bonders. CO is a strong π-acceptor. The strength of ligand field increases in the order THF < Py ≈ Im < CO. On the basis of the ^{19}F NMR spectroscopic studies,[5] the $CoTPPF_{28}(L)_2$ complexes with L = THF and Py have partial population of the high-spin state; when L is 1-methylimidazole (1-MeIm), its coordination leads to complete conversion to the high-spin state. No experimental results are available for $CoTPPF_{28}(CO)_2$. It is interesting to compare the electronic structures of the various $CoTPPF_x(L)_2$ complexes with different types of axial ligands, where we used a simpler Im ligand to mimic the actual 1-MeIm ligand. Furthermore, other properties such as binding energies, ionization potentials, and electron affinities are computed; they also provide sensitive probes of the electronic effects of the peripheral substituents and of the axial ligands in the metal porphyrins.

An accurate description of the electronic structure and bonding in several first-row transition metal compounds (e.g., those containing Cr, Mn, Fe, Co, Ni) has proven to be a challenge to theoretical researchers because of the existence of a number of low-lying states which prevent simple determination of the ground states of the systems. The Hartree−Fock (HF) method is inadequate, as it does not account for electron correlation. Ab initio studies require the use of high-quality correlated methods, but most of those methods are very computationally expensive and impractical for large molecular systems.

Another nonempirical approach that has proven to be quite a useful tool in studying compounds of transition metals is the density functional theory (DFT); it provides an estimate of the correlation energy at a relatively modest cost. However, the DFT methods depend on an adequate exchange-correlation (XC) potential. By a series of educated trials and errors, more and more accurate XC forms have been developed. A "good" XC functional now consists of two parts: LDA (local density approximation) and GGA (generalized gradient approximation) corrections. The former is obtained mainly from the cases of a homogeneous electron gas. Further progress in DFT is the introduction of a fraction of exact HF-type exchange;[10] the resulting formulas are often referred to as "hybrid" functionals, and it has been shown that the exact-exchange mixing leads to a significant improvement in the performance of DFT.

There are, however, disadvantages to using exact exchange; it considerably increases the computing effort. Recently, some attempts were made to replace the exact-exchange part of hybrid DFTs with a pure density functional part. On the basis of the density matrix expansion for the exchange functional, van Voorhis and Scuseria[11] developed a new approximate XC form by including the electron kinetic energy density τ [$=\Sigma(\nabla\phi_i)^2$]. Such a form is called meta-GGA, which does not contain exact exchange. The authors[11] show that τ is a good alternative to exact-exchange mixing. Later, some other τ-dependent functionals were reported[12,13] and were shown to perform comparably to hybrid functionals.

Meanwhile, great efforts have also been made in recent years in order to obtain optimum GGA functionals. Perdew, Burke, and Ernzerhof (PBE)[14] suggested a simplified GGA, in which all the parameters are fundamental constants. Then, revised or modified versions of the PBE exchange functional have been proposed by several research groups.[15−17] Hamprecht, Cohen, Tozer, and Handy derived a GGA functional which contains 15 parameters.[18] (The resulting functional is denoted as HCTH.) These parameters were first refined against data from a training set of 93 atomic and molecular systems.[18] Then, the training set was extended to 120, 147, and 407 systems.[19] Later, Boese and Handy[13] introduced the variable τ into HCTH, giving a new functional τ-HCTH.

Although the recently developed functionals yield satisfactory numerical results for a wide variety of chemical applications, they have been tested only on a series of small molecules that contain mainly main-group elements. It is still unclear that a density functional successful for one system will be equally useful for different systems, particularly for transition-metal compounds[20] and chemical reactions.[21] For FePor(Cl), for example, the density functionals used meet difficulties in calculating the energetics of the high-spin state.[20] Another purpose of this work is to examine the performance of a variety of density functionals on the electronic structure of the $CoTPPF_x(L)_2$ compounds, including a meta-GGA (τ-HCTH) and a hybrid (B3LYP) functional.

2. Computational Details

The molecular structure of $CoTPPF_x$ is illustrated in Figure 1. For computational purposes, the symmetry and geometry of the molecule are of importance. X-ray crystal structure data of $CoTPPF_{28}(toluene)_2$ and $CoTPPF_{28}(THF)_2$ indicate that the macrocycle is nearly planar with essentially orthogonal phenyl groups.[5] The same is true for CoTPP in the solid state (slightly ruffled).[22] Since the H atom is smaller than F, we expect that the geometry will not change for steric reasons when the F atoms in $CoTPPF_{28}$ are replaced by H atoms in $CoTPPF_8$ and $CoTPPF_{20}$. Therefore, all the $CoTPPF_x$ systems were assumed to belong to the D_{4h} point group. The four phenyl groups of $TPPF_x$ were assumed to be perpendicular to the porphyrin plane, as shown by experiments.[5] To examine the influence of ruffling on the properties of $CoTPPF_x$, we give, in the Supporting Information (Table S1), a comparison of the calculated properties of the optimized D_{2d} (ruffled) and D_{4h} (square planar) structures. It is shown that the deviation from perpendicularity has only a minor effect on the calculated properties. The energies differ by 0.02−0.04 eV, and the lengths of the Co−N bond differ by less than 0.005 Å. Ionization potentials are scarcely affected at all, nor are the electron affinities. Indeed, our finding of only minor perturbations is consistent with previous calculations.[23a,b]

All calculations were carried out using the Amsterdam density functional (ADF) program package (version 2004.01).[24−27] The density functionals[10,13−19,28−33] chosen for testing are listed in Table 1, together with a brief description of their formulation. In the present version of ADF, many meta-GGA and hybrid-

TABLE 1: Functionals Used in the Calculations

functional	formulation
VWN−B−P	Vosko-Wilk-Nusair's 1980 local correlation functional (ref 28) plus Becke's 1988 gradient correction for exchange (ref 29) and Perdew's 1986 gradient correction for correlation (ref 30).
mPW	Modified Perdew-Wang's 1991 exchange functional plus Perdew-Wang's 1991 correlation functional (containing both local and GGA terms) (ref 31).
PBE	Perdew-Burke-Ernzerhof's 1996 corrections for both exchange and correlation (ref 14).
revPBE	Revised PBE functional proposed in 1998 by Zhang-Yang (ref 15).
RPBE	Revised PBE functional proposed in 1999 by Hammer-Hansen-Nørskov (ref 16).
mPBE	Modified PBE functional proposed in 2002 by Adamo and Barone (ref 17).
OPBE	Handy-Cohen's 2001 OPTX correction for exchange (ref 32) plus Perdew-Burke-Ernzerhof's 1996 correction for correlation.
OLYP	Handy-Cohen's 2001 OPTX correction for exchange plus Lee−Yang−Parr's 1988 correlation functional (containing both local and GGA terms) (ref 33).
HCTH/407	Hamprecht-Cohen-Tozer-Handy 1998 correction for both exchange and correlation (ref 18), containing 15 parameters refined against data from a training set of 407 atomic and molecular systems (ref 19).
τ-HCTH	The kinetic-energy density τ [$=\Sigma(\nabla\phi_i)^2$] is included in the HCTH/407 form (ref 13).
B3LYP	Becke's 1993 three-parameter hybrid functional (ref 10) using Lee−Yang−Parr's 1988 correlation functional.

GGA functionals have also been implemented, but they are treated in a non-self-consistent (non-SCF) manner. That is, the SCF equations are solved at the LDA level; then, the obtained LDA densities are used as input for another non-SCF GGA energy evaluation. For a given molecular structure, non-SCF and SCF procedures are shown to yield nearly the same relative energies (see section 3.1). Because these functionals do not have an implementation for the XC potential, geometry optimizations and calculations on some properties cannot be performed with them. In our calculations, the molecular structures are optimized using the VWN-B-P functional. It has been shown that the usage of non-SCF energies evaluated at constant structure can be made without notable loss of accuracy.[16] Generally, DFT (e.g., the used VWN-B-P) gives an excellent description of molecular structure of a given electronic state for transition-metal systems (although it may be unsuccessful in describing the energetics of the particular electronic state, e.g., the high-spin state).[20] The changes in calculated molecular structure by using different functionals are in fact small and do not produce notable errors in the calculated energies (see next section).

The STO basis set employed is the standard ADF-TZP which is triple-ζ for valence orbitals plus one polarization function. To obtain accurate results, the valence set on Co included subvalence 3s and 3p shells. For C, N, F, and O, 2s and 2p were considered valence shells. The other shells of lower energy, i.e., [Ne] for Co and [He] for C/N/F/O, were described as core and kept frozen according to the frozen core approximation.[24] This is shown to yield results quite similar to those obtained by all-electron calculations (see Supporting Information, Table S2). Relativistic corrections of the valence electrons were calculated by the quasi-relativistic (QR) method.[34] For the open-shell states, the unrestricted Kohn−Sham (KS) spin-density functional approach was adopted.

The ionization potentials (IPs) and electron affinities (EAs) were calculated by the so-called ΔSCF method in which separate SCF calculations for the neutral molecule and its ion are carried out and $EA = E(X^-) - E(X)$.

It should be understood that the calculations deal specifically with free molecules, i.e., gas phase, while the experimental results relate to the solid or solution. To assess the effects of solvent on the binding of axial ligands to the metal porphyrins, calculations were performed on $CoTPP(THF)_2$ in dichloromethane (CH_2Cl_2, dielectric constant $\epsilon = 8.93$). A comparison of the calculated properties between the free molecule and the molecule in the solvent is provided in the Supporting Information (Table S3). Upon solvation, there are nearly no changes in the equatorial Co−N and axial Co−O bond lengths. But the $CoTPP-(THF)_2$ binding energy is decreased by 0.1 eV, owing to the greater stabilizations of the isolated components. The ionization potential is decreased significantly, and the electron affinity is greatly increased. These results indicate that the positive or negative ion is strongly stabilized by the polar solvent.

3. Results and Discussion

Placing the molecule in the *xy* plane, the five Co 3d orbitals transform as a_{1g} (d_{z^2}), b_{1g} ($d_{x^2-y^2}$), e_g (d_π, i.e., d_{xz} and d_{yz}), and b_{2g} (d_{xy}). Different occupations of electrons in these d orbitals can yield a number of possible low-lying electronic states. To determine the ground state, relative energies of two low-spin ($S = {}^1/_2$) and two high-spin ($S = {}^3/_2$) configurations for every Co complex were calculated. Geometry optimization was performed separately for each configuration considered.

We first examined effects of different density functionals on the molecular structures of the selected configurations. CoTPP was taken as a prototype. The structural and energetic results from fully self-consistent calculations with the VWN-B-P, mPW, RPBE, OPBE, and OLYP functionals are presented in Table 2. It is shown that all these functionals yield very similar Co−N bond lengths for every electronic configuration; they are in the range 1.96−1.98 Å for $^2A_{1g}$, 1.95−1.97 Å for ^2E_g, 2.03−2.05 Å for $^4A_{2g}$, and 2.02−2.04 Å for ^4E_g. The calculated Co−N bond lengths in the ground state ($^2A_{1g}$) compare favorably with the experimental value of 1.95 Å measured in the solid state.[22] Although the molecular structures show little dependence on the choice of the XC functionals, the calculated relative energies of the states are sensitive to them. For example, the relative energy of $^4A_{2g}$ obtained with VWN-B-P is 1.17 eV, which is 0.3 eV larger than the corresponding value obtained with OLYP. But the small changes in the molecular structure have negligible effect on the calculated relative energies. This is evident from the values in Table 3**.**

3.1. $CoTPPF_x$ ($x = 0, 8, 20, 28$). To better understand effects of axial ligands on the electronic structure of the cobalt porphyrins, the various unligated $CoTPPF_x$ systems are investigated as well. Table 3 presents the results for the relative energies ($E^{relative}$) of the four selected electronic states, calculated with the various density functionals non-self-consistently on the basis of the self-consistent VWN-B-P calculations at the VWN-B-P structures. Comparing the data of Table 2 with the corresponding data in Table 3, we see that the non-SCF and SCF values of $E^{relative}$ for each functional considered are very similar.

The ground state of CoTPP is known to be $^2A_{1g}$ [$(d_{xy})^2(d_{z^2})^1(d_\pi)^4$] from analysis of the ESR spectra.[35] The calculations are consistent with this assignment. The ^2E_g state, arising from the $(d_{xy})^2(d_{z^2})^2(d_\pi)^3$ configuration, lies 0.2−0.3 eV higher in energy. Except for B3LYP,[36] all other density functionals yield similar results for the relative energy of ^2E_g. The substituted $CoTPPF_x$ systems have the same $^2A_{1g}$ ground state as CoTPP. Although the ^2E_g relative energy does not change very much from one system to another, a general trend can be found. The $E^{relative}$ of ^2E_g is about 0.03 eV smaller in $CoTPPF_8$ and $CoTPPF_{28}$ than

TABLE 2: Calculated Relative Energies (*E*, eV) for Selected States of CoTPP with Various Density Functionals

	E^{relative} ($R_{\text{Co-N(eq)}}$)[a]			
	$^2A_{1g}$ ($b_{2g}^2a_{1g}^1e_g^4$)[b]	^2E_g ($b_{2g}^2a_{1g}^2e_g^3$)	$^4A_{2g}$ ($b_{2g}^1a_{1g}^1e_g^4b_{1g}^1$)	^4E_g ($b_{2g}^2a_{1g}^1e_g^3b_{1g}^1$)
VWN−B−P	0 (1.972)	0.23 (1.960)	1.17 (2.035)	1.35 (2.023)
mPW	0 (1.973)	0.24 (1.960)	1.16 (2.036)	1.37 (2.025)
RPBE	0 (1.984)	0.27 (1.973)	0.98 (2.049)	1.22 (2.038)
OPBE	0 (1.962)	0.33 (1.950)	0.90 (2.026)	1.07 (2.015)
OLYP	0 (1.977)	0.27 (1.968)	0.87 (2.042)	1.06 (2.030)
exptl[c]	0 (1.949)			

[a] Values in parentheses are the optimized equatorial Co−N(eq) bond length (in Å) for the pertinent state. [b] Orbital energy levels illustrated in Figure 2, where $b_{2g} \approx d_{xy}$, $a_{1g} \approx d_{z^2}$, $1e_g \approx d_\pi$, and $b_{1g} \approx d_{x^2-y^2}$. [c] Ref 22.

TABLE 3: Calculated Relative Energies (*E*, eV) for Selected States of $CoTPPF_x$ ($x = 0, 8, 20, 28$) and $CoOTPF_{28}$ with Various Density Functionals

		E^{relative}, eV				
	state	CoTPP	$CoTPPF_8$	$CoTPPF_{20}$	$CoTPPF_{28}$	$CoOTPF_{28}$
VWN−B−P	$^2A_{1g}$	0 (1.972)[a]	0 (1.986)	0 (1.973)	0 (1.988)	0 (2.020)
	^2E_g	0.23 (1.960)	0.20 (1.973)	0.26 (1.960)	0.22 (1.976)	0.34 (2.009)
	$^4A_{2g}$	1.17 (2.035)	1.05 (2.048)	1.15 (2.035)	1.04 (2.049)	0.75 (2.087)
	^4E_g	1.35 (2.023)	1.10 (2.035)	1.32 (2.023)	1.09 (2.036)	0.90 (2.076)
exptl	$^2A_{1g}$	0 (1.949)[b]			0 (1.986)[c]	
mPW	$^2A_{1g}$	0	0	0	0	0
	^2E_g	0.25	0.22	0.27	0.24	0.36
	$^4A_{2g}$	1.18	1.05	1.17	1.01	0.74
	^4E_g	1.37	1.11	1.36	1.08	0.92
PBE	$^2A_{1g}$	0	0	0	0	0
	^2E_g	0.21	0.18	0.24	0.20	0.33
	$^4A_{2g}$	1.17	1.04	1.16	1.01	0.74
	^4E_g	1.34	1.08	1.33	1.05	0.89
revPBE	$^2A_{1g}$	0	0	0	0	0
	^2E_g	0.26	0.24	0.27	0.25	0.36
	$^4A_{2g}$	1.05	0.91	1.03	0.88	0.60
	^4E_g	1.26	0.98	1.23	0.96	0.79
RPBE	$^2A_{1g}$	0	0	0	0	0
	^2E_g	0.27	0.24	0.28	0.26	0.37
	$^4A_{2g}$	1.01	0.87	0.99	0.84	0.55
	^4E_g	1.23	0.95	1.20	0.94	0.76
mPBE	$^2A_{1g}$	0	0	0	0	0
	^2E_g	0.23	0.20	0.25	0.22	0.34
	$^4A_{2g}$	1.12	0.99	1.11	0.96	0.68
	^4E_g	1.31	1.05	1.30	1.02	0.86
OPBE	$^2A_{1g}$	0	0	0	0	0
	^2E_g	0.32	0.28	0.35	0.30	0.42
	$^4A_{2g}$	0.95	0.81	0.95	0.76	0.47
	^4E_g	1.10	0.84	1.10	0.79	0.61
OLYP	$^2A_{1g}$	0	0	0	0	0
	^2E_g	0.27	0.24	0.29	0.26	0.36
	$^4A_{2g}$	0.92	0.79	0.91	0.74	0.45
	^4E_g	1.10	0.84	1.09	0.80	0.62
HCTH/407	$^2A_{1g}$	0	0	0	0	0
	^2E_g	0.17	0.14	0.19	0.15	0.25
	$^4A_{2g}$	0.81	0.69	0.80	0.64	0.34
	^4E_g	0.96	0.70	0.96	0.68	0.48
τ-HCTH	$^2A_{1g}$	0	0	0	0	0
	^2E_g	0.16	0.13	0.18	0.14	0.26
	$^4A_{2g}$	0.60	0.47	0.58	0.44	0.18
	^4E_g	0.71	0.46	0.69	0.42	0.28
B3LYP	$^2A_{1g}$	0	0	0	0	
	$^4A_{2g}$	0.57	0.50	0.56	0.44	

[a] Values in parentheses are the optimized equatorial Co−N(eq) bond length (in Å) for the pertinent state. [b] Ref 22. [c] Ref 5.

in CoTPP and $CoTPPF_{20}$ (where CoTPP ≈ $CoTPPF_{20}$ and $CoTPPF_8 \approx CoTPPF_{28}$). That is, only the direct substitution at the β-pyrrole position has an effect on the relative energy of ^2E_g.

The relative energies of the high-spin states $^4A_{2g}$ and ^4E_g are significantly larger than that of ^2E_g, and they are, however, rather dependent upon the method used. For $^4A_{2g}$ in CoTPP, most GGA functionals yield an E^{relative} which is more than 1 eV. A smaller E^{relative} of ∼0.9 eV is obtained by OPBE or OLYP, whereas a value of ∼0.8 eV is given by HCTH/407. By including τ into the HCTH functional, the E^{relative} decreases to 0.60 eV. The hybrid functional B3LYP gives a very comparable result (0.57 eV) to τ-HCTH. The same is true for the other $CoTPPF_x$ systems. This suggests that the τ-form in the τ-HCTH functional is indeed able to simulate exact HF-type exchange.

The results also show how the peripheral substitution influences the relative energies of the high-spin states. From CoTPP to $CoTPPF_8$ or from $CoTPPF_{20}$ to $CoTPP_{28}$, the E^{relative} decreases

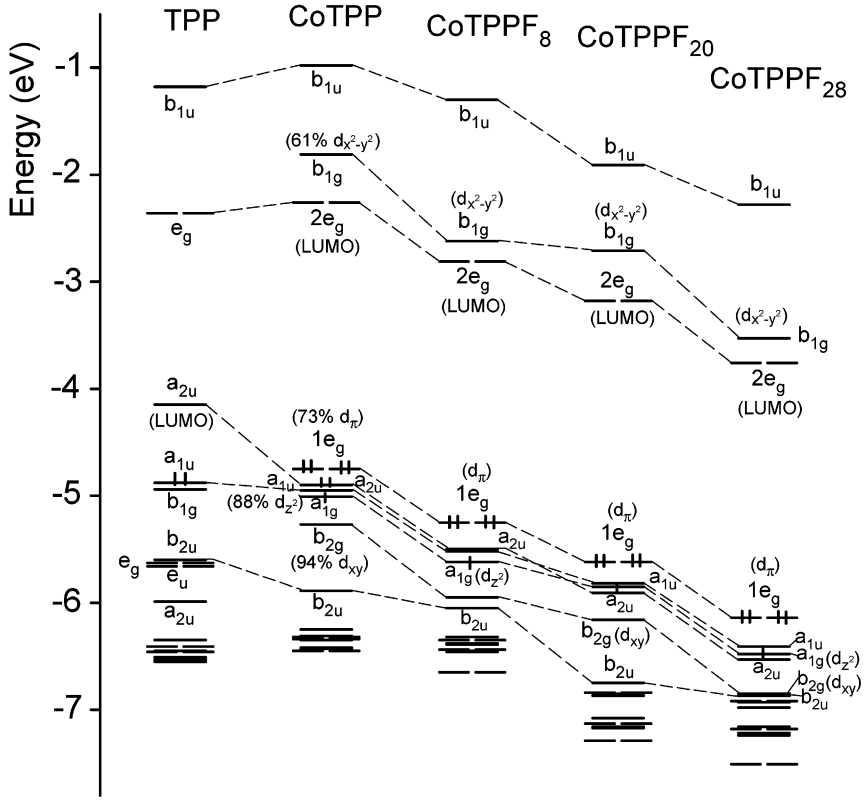

Figure 2. Orbital energy levels of TPP (on the left, with no H atoms in the ring cage) and the various substituted cobalt tetraphenylporphyrins.

notably, by ~0.15 eV. However, almost no change or a very small decrease in E^{relative} is found from CoTPP to $CoTPPF_{20}$ or from $CoTPPF_8$ to $CoTPPF_{28}$. Therefore, the electron-withdrawing substituents at the *meso*-phenyl positions have little influence on the electronic state of $CoTPPF_x$.

The $^4A_{2g}-{}^4E_g$ energy gap in CoTPP/$CoTPPF_{20}$ is 0.1−0.2 eV, depending on the density functional used; it is smaller, 0−0.1 eV, in $CoTPPF_8$/$CoTPPF_{28}$. According to the τ-HCTH results, the $^4A_{2g}$ and ^4E_g states in $CoTPPF_{28}$ are nearly degenerate and lie ~0.4 eV above the ground state.

We also calculated a hypothetical compound, cobalt octakis(perfluoro *i*-CF_3)tetrafluoroporphyrin, $CoOTPF_{28}$, where the eight β-pyrrole F atoms and four *meso*-phenyl groups in $CoTPPF_{28}$ are replaced by the CF_3 groups and F atoms. As CF_3 is a more electronegative than F, $OTPF_{28}$ should be an even more electron-deficient ligand than $TPPF_{28}$. Then, from $CoTPPF_{28}$ to $CoOTPF_{28}$, there is a significant Co−N bond expansion, accompanied by a further decrease of ~0.3 eV in the relative energy of $^4A_{2g}$. Nevertheless, the lowest quartet $^4A_{2g}$ in $CoOTPF_{28}$ still lies ~0.2 eV above the ground state based on the τ-HCTH results.

Figure 2 illustrates the valence molecular orbital (MO) energy levels for the ground states of the four $CoTPPF_x$ molecules. The interaction between Co and $TPPF_x$ splits the metal 3d orbitals greatly. The d_{z^2} and d_π orbitals are weakly antibonding, higher in energy than the nonbonding d_{xy}. The unoccupied b_{1g} ($d_{x^2-y^2}$) is strongly antibonding, lying above the LUMO $2e_g$ (π^*). Fluoro-substitution has a lowering effect on the MOs. From CoTPP to $CoTPPF_8$ or from $CoTPPF_{20}$ to $CoTPPF_{28}$, the $d_{x^2-y^2}$ orbital is lowered to a larger extent than other MOs, whereas the b_{2u} orbital is lowered only slightly. However, nearly uniform downshifts of the MOs can be seen from CoTPP to $CoTPPF_{20}$ or from $CoTPPF_8$ to $CoTPPF_{28}$. The MO energy level diagrams again indicate that CoTPP is similar to $CoTPPF_{20}$ and $CoTPPF_8$ is similar to $CoTPPF_{28}$. They can also explain why the relative energies of the high-spin states in CoTPP/$CoTPPF_{20}$ are larger than those in $CoTPPF_8$/$CoTPPF_{28}$.

3.2. $CoTPPF_x(L)_2$. We now examine effects of a pair of axial ligands (L) upon the electronic structure of the cobalt porphyrins. The $CoTPPF_x(L)_2$ complexes with L = THF, Py, and Im were constructed by attaching each ligand to Co with the O or N atom pointing toward the metal; the molecular plane of the ligand was perpendicular to the porphyrin, bisecting its N−Co−N angles. This geometry has been observed in the X-ray crystal structure.[5] With L = CO, each ligand was attached to the central metal with Co−C−O in a linear arrangement, perpendicular to the porphyrin plane. $CoTPPF_x(CO)_2$ retains the D_{4h} symmetry of the unligated $CoTPPF_x$, while the symmetries of the other $CoTPPF_x(L)_2$ complexes are reduced to D_{2h}.

The perturbations caused by the L ligands in the MO energy-level diagrams of $CoTPPF_x$ ($x = 0, 28$) are illustrated in Figure 3. By comparing CoTPP to $CoTPP(THF)_2$, an obvious effect of the axial ligands is to dramatically raise the energy of the Co a_{1g} (d_{z^2}) orbital, attributable to the strong repulsive interaction between the axial−ligand HOMO and the metal d_{z^2}. The $1e_g$ (d_π) orbitals are split into $1b_{2g}$ (d_{xz}) and $1b_{3g}$ (d_{yz}), which are, however, only narrowly separated. For the ligated complexes, the possible low-lying states are now, in D_{2h} symmetry, $^2A_{1g}$, $^4B_{3g}$ (or equivalently $^4B_{2g}$), and $^4B_{1g}$, which correspond to the unligated complexes' $^2A_{1g}$, ^4E_g, and $^4A_{2g}$ states, respectively. The ^2E_g [$(d_{xy})^2(d_{z^2})^2(d_\pi)^3$] state was not considered; our calculations show that the presence of two electrons in the d_{z^2} orbital prevents close association of any axial ligands. Table 4 displays the VWN-B-P optimized bond lengths ($R_{\text{Co-N(eq)}}$ and $R_{\text{Co-L(ax)}}$) for the selected states in each $CoTPPF_x(L)_2$ complex. (The results for the $^4B_{2g}$ state are not given, as they are nearly equal to those of $^4B_{3g}$). For convenience, we use the D_{4h} term symbols

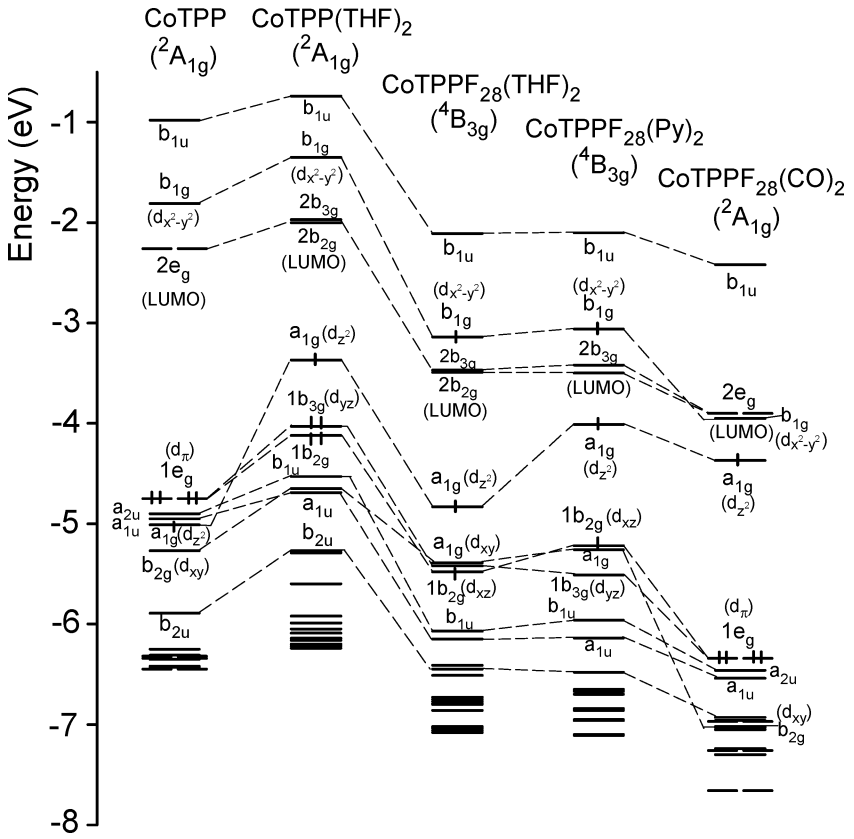

Figure 3. Orbital energy levels of CoTPP and CoTPPF$_{28}$ when complexed with two axial ligands L (L = THF, Py, CO).

TABLE 4: Optimized Equatorial Co−N(eq) and Axial Co−L(ax) Bond Lengths (*R* in Å) for Selected States of CoTPPF$_x$(L)$_2$ (*x* = 0, 8, 20, 28; L = THF, Py, Im, CO) with the VWN-B-P Functional

		x = 0		*x* = 8		*x* = 20		*x* = 28	
	state	$R_{Co-N(eq)}$	$R_{Co-L(ax)}$	$R_{Co-N(eq)}$	$R_{Co-L(ax)}$	$R_{Co-N(eq)}$	$R_{Co-L(ax)}$	$R_{Co-N(eq)}$	$R_{Co-L(ax)}$
L = THF	$^2A_{1g}$ ($^2A_{1g}$)[a]	1.980	2.395	1.995	2.385	1.980	2.386	1.998	2.376
	$^4B_{3g}$[b](^4E_g)	2.038	2.358	2.051	2.349	2.043	2.300	2.057	2.332
	$^4B_{1g}$ ($^4A_{2g}$)	2.045	2.378	2.062	2.363	2.041	2.321	2.055	2.354
exptl[c]	$^4B_{3g}$ (^4E_g)							2.068	2.204
L = Py	$^2A_{1g}$ ($^2A_{1g}$)	1.986	2.307	2.000	2.308	1.986	2.312	2.001	2.302
	$^4B_{3g}$ (^4E_g)	2.040	2.293	2.054	2.294	2.038	2.305	2.060	2.281
	$^4B_{1g}$ ($^4A_{2g}$)	2.051	2.295	2.066	2.295	2.052	2.299	2.070	2.304
L = Im	$^2A_1$ ($^2A_{1g}$)	1.988	2.265	2.000	2.273	1.989	2.277	2.011	2.264
	$^4B_1$ (^4E_g)	2.049	2.217	2.064	2.218	2.048	2.216	2.073	2.199
	$^4B_2$ ($^4A_{2g}$)	2.045	2.242	2.062	2.221	2.059	2.218	2.075	2.210
L = CO	$^2A_{1g}$	2.010	2.040					2.034	2.045
	^4E_g	2.061	2.049					2.087	2.046
	$^4A_{2g}$	2.075	2.029					2.100	2.035

[a] State in parentheses refers to the corresponding designation in unligated CoTPPF$_x$. [b] The results for the $^4B_{2g}$ state are not given, as they are nearly equal to those of $^4B_{3g}$. [c] Ref 5.

also for the lower symmetry systems in the following discussion of the results.

3.2.1. L = THF. The calculated relative energies for the selected states in CoTPPF$_x$(THF)$_2$ (x = 0, 8, 20, 28) with the various density functionals are presented in Table 5. Examining the VWN-B-P results first, we see that the relative energies of the high-spin states in the ligated complex are significantly smaller than those in the unligated one. The magnitudes of the energy decrease are about 0.2 and 0.5 eV for the $^4A_{2g}$ and ^4E_g states, respectively. Therefore, the energy ordering between $^4A_{2g}$ and ^4E_g is reversed in the ligated complex. Similar situations are also found with other density functionals used. That is, the coordination of the two axial ligands leads to a systematic decrease in the high-spin state's relative energy, regardless of the density functional used. To facilitate comparison of the calculated relative energies of ^4E_g among the different CoTPPF$_x$-(THF)$_2$ species and the various functionals, plots of $E^{relative}$ versus x and DFT method are shown in Figure 4, together with the results for CoTPPF$_x$ obtained by the VWN-B-P functional. The $E^{relative}$ clearly shows a zigzag variation on going from x = 0 to x = 28. The energy gap between the dotted and solid VWN-B-P lines reflects the effect of the axial THF ligands to decrease the relative energy of the high-spin state, and the energy ordering from one functional to another reflects the relative performances of the functionals in describing the energetics of the high-spin state.

According to the τ-HCTH results, the ground state of CoTPPF$_{28}$(THF)$_2$ is high-spin, consistent with the experimental observation.[5] Further ^{19}F NMR spectroscopic studies[5] have suggested that the most likely ground state for this compound

TABLE 5: Calculated Relative Energies (*E*, eV) for Selected States of $CoTPPF_x(THF)_2$ ($x = 0, 8, 20, 28$) with Various Density Functionals

		$E^{relative}$ [in $CoTPPF_x(THF)_2$]			
	state	$x = 0$	$x = 8$	$x = 20$	$x = 28$
VWN−B−P	$^2A_{1g}$ ($^2A_{1g}$)[a]	0	0	0	0
	$^4B_{3g}$ (^4E_g)	0.84	0.61	0.77	0.55
	$^4B_{1g}$ ($^4A_{2g}$)	0.98	0.84	0.96	0.82
mPW	$^2A_{1g}$ ($^2A_{1g}$)	0	0	0	0
	$^4B_{3g}$ (^4E_g)	0.85	0.62	0.80	0.53
	$^4B_{1g}$ ($^4A_{2g}$)	0.99	0.85	0.98	0.79
PBE	$^2A_{1g}$ ($^2A_{1g}$)	0	0	0	0
	$^4B_{3g}$ (^4E_g)	0.84	0.61	0.78	0.52
	$^4B_{1g}$ ($^4A_{2g}$)	0.98	0.84	0.96	0.78
revPBE	$^2A_{1g}$ ($^2A_{1g}$)	0	0	0	0
	$^4B_{3g}$ (^4E_g)	0.74	0.51	0.70	0.41
	$^4B_{1g}$ ($^4A_{2g}$)	0.88	0.73	0.87	0.66
RPBE	$^2A_{1g}$ ($^2A_{1g}$)	0	0	0	0
	$^4B_{3g}$ (^4E_g)	0.71	0.47	0.67	0.38
	$^4B_{1g}$ ($^4A_{2g}$)	0.84	0.69	0.84	0.62
mPBE	$^2A_{1g}$ ($^2A_{1g}$)	0	0	0	0
	$^4B_{3g}$ (^4E_g)	0.81	0.57	0.75	0.48
	$^4B_{1g}$ ($^4A_{2g}$)	0.94	0.80	0.93	0.73
OPBE	$^2A_{1g}$ ($^2A_{1g}$)	0	0	0	0
	$^4B_{3g}$ (^4E_g)	0.64	0.39	0.64	0.30
	$^4B_{1g}$ ($^4A_{2g}$)	0.77	0.60	0.80	0.54
OLYP	$^2A_{1g}$ ($^2A_{1g}$)	0	0	0	0
	$^4B_{3g}$ (^4E_g)	0.63	0.39	0.63	0.30
	$^4B_{1g}$ ($^4A_{2g}$)	0.75	0.59	0.78	0.53
HCTH/407	$^2A_{1g}$ ($^2A_{1g}$)	0	0	0	0
	$^4B_{3g}$ (^4E_g)	0.56	0.31	0.54	0.23
	$^4B_{1g}$ ($^4A_{2g}$)	0.65	0.49	0.68	0.43
τ-HCTH	$^2A_{1g}$ ($^2A_{1g}$)	0	0	0	0
	$^4B_{3g}$ (^4E_g)	0.25	0.01	0.19	−0.09
	$^4B_{1g}$ ($^4A_{2g}$)	0.39	0.24	0.36	0.17

[a] State in parentheses refers to the corresponding designation in unligated $CoTPPF_x$.

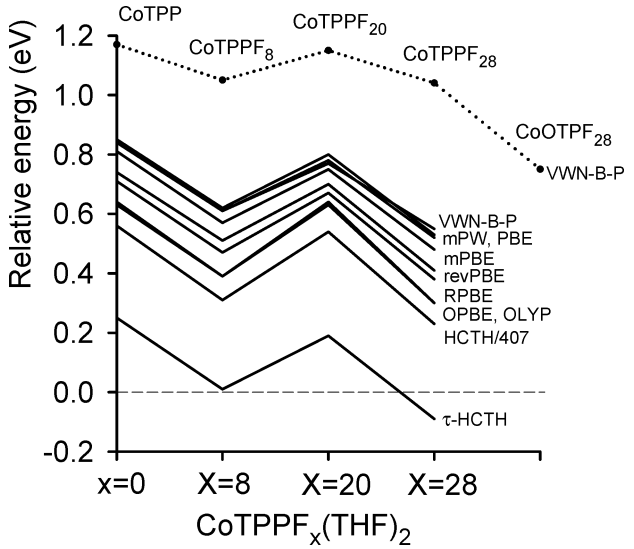

Figure 4. Schematic illustration of the relative energies of the high-spin $^4B_{2g}$ (^4E_g) state (which is relative to the energy of $^2A_{1g}$) in the $CoTPPF_x(THF)_2$ complexes ($x = 0, 8, 20, 28$), obtained with the various density functionals. The upper dotted line represents the relative energy of $^4A_{2g}$ $[(d_{xy})^1(d_{z^2})^1(d_\pi)^4(d_{x^2-y^2})^1]$ in the unligated $CoTPPF_x$ and $CoOTPF_{28}$ systems.

is ^4E_g, which is confirmed by the calculations as well. The low-spin $^2A_{1g}$ is now the second lowest state, 0.09 eV higher in energy. Since the energy gap between $^2A_{1g}$ and ^4E_g is so small, this may explain why the ^4E_g state is not fully populated in $CoTPPF_{28}(THF)_2$.

TABLE 6: Calculated Relative Energies (*E*, eV) for Selected States of $CoTPPF_x(L)_2$ ($x = 0, 8, 20, 28$; L = Py, Im, CO) with the VWN-B-P and τ-HCTH Functionals

		$E^{relative}$			
	state	$x = 0$	$x = 8$	$x = 20$	$x = 28$
	(a) in $CoTPPF_x(Py)_2$				
VWN−B−P	$^2A_{1g}$ ($^2A_{1g}$)[a]	0	0	0	0
	$^4B_{3g}$ (^4E_g)	0.89	0.65	0.85	0.62
	$^4B_{1g}$ ($^4A_{2g}$)	0.94	0.79	0.92	0.77
τ-HCTH	$^2A_{1g}$ ($^2A_{1g}$)	0	0	0	0
	$^4B_{3g}$ (^4E_g)	0.27	0.02	0.21	−0.05
	$^4B_{1g}$ ($^4A_{2g}$)	0.32	0.16	0.27	0.10
	(b) in $CoTPPF_x(Im)_2$				
VWN−B−P	$^2A_1$ ($^2A_{1g}$)[a]	0	0	0	0
	$^4B_1$ (^4E_g)	0.85	0.59	0.80	0.50
	$^4B_2$ ($^4A_{2g}$)	0.90	0.73	0.88	0.63
τ-HCTH	$^2A_1$ ($^2A_{1g}$)	0	0	0	0
	$^4B_1$ (^4E_g)	0.25	−0.02	0.18	−0.12
	$^4B_2$ ($^4A_{2g}$)	0.28	0.10	0.24	0.02
	(c) in $CoTPPF_x(CO)_2$				
VWN−B−P	$^2A_{1g}$	0			0
	^4E_g	1.33			1.03
	$^4A_{2g}$	1.03			0.89
τ-HCTH	$^2A_{1g}$	0			0
	^4E_g	0.72			0.39
	$^4A_{2g}$	0.45			0.28

[a] State in parentheses refers to the corresponding designation in unligated $CoTPPF_x$.

The pure density functionals without τ show more or less overestimation (too positive) of relative energy of the high-spin state, where HCTH/407 gives comparatively the best results among these functionals. On the other hand, the τ-HCTH functional yields significantly improved energy as compared to HCTH/407; a rather large energy gap between the τ-HCTH and HCTH/407 lines can be seen in Figure 4.

In the case of $CoTPPF_8(THF)_2$, the τ-HCTH results show the ground state to be either $^2A_{1g}$ or ^4E_g; their energies are too close to distinguish. Both $CoTPP(THF)_2$ and $CoTPPF_{20}(THF)_2$ still have a low-spin $^2A_{1g}$ state, while the high-spin state (^4E_g) lies 0.2−0.3 eV higher in energy.

3.2.2. L = Py, Im, or CO. Table 6 contains the calculated relative energies for selected states in the other ligated $CoTPPF_x(L)_2$ complexes with L = Py, Im, or CO. Here, only the VWN-B-P and τ-HCTH results have been presented. The results obtained by the other density functionals are given in the Supporting Information (Tables S4−S6). In fact, the magnitude of the change in the high-spin state $E^{relative}$ from one density functional to another is nearly the same for the different systems. That is, there is a systematic shift of the energy lines in Figure 4 when L is different from THF.

The τ-HCTH results also indicate a ^4E_g ground state for $CoTPPF_{28}(Py)_2$, again in agreement with the experimental observation.[5] But the energy separation (0.05 eV) between the $^2A_{1g}$ and ^4E_g states in this complex is slightly smaller than that in $CoTPPF_{28}(THF)_2$, and so, one may expect more population of the low-spin state for $CoTPPF_{28}(Py)_2$. With L = Im, the relative energy of ^4E_g is decreased by 0.03 eV as compared to $CoTPPF_{28}(THF)_2$, indicating that the Im ligand favors a more stable high-spin state than THF. The ^{19}F NMR studies[5] showed a complete conversion to the ^4E_g state in $CoTPPF_{28}(1\text{-MeIm})_2$. The trend in the calculated results is in agreement with the experimental observation. However, the very small decrease in the $E^{relative}$ from L = THF to L = Im may not convincingly account for the difference between $CoTPPF_{28}(THF)_2$ and $CoTPPF_{28}(1\text{-MeIm})_2$. Probably, the electronic effect of 1-MeIm cannot be simulated fully by the simpler Im ligand.

TABLE 7: Calculated Properties[a] for Unligated CoTPPF$_x$ Complexes (x = 0, 8, 20, 28) in Their Ground State ($^2A_{1g}$), with the VWN-B-P (func1) and τ-HCTH (func2) Functionals

		CoTPP		$CoTPPF_8$		$CoTPPF_{20}$		$CoTPPF_{28}$	
		func1	func2	func1	func2	func1	func2	func1	func2
$R_{Co-N(eq)}$, Å		1.972		1.986		1.973		1.988	
E_{bind}, eV		10.90	9.78	10.45	9.34	11.17	9.96	10.75	9.63
IP[b], eV	$1e_g/d_\pi$	6.73	6.61	**7.08**	**6.96**	7.47	7.35	**7.75**	**7.63**
	a_{2u}	**6.56**	**6.53**	7.11	7.07	7.48	7.43	8.05	7.97
	a_{1u}	6.63	6.57	7.18	7.11	**7.42**	**7.34**	7.91	7.82
EA[b], eV	a_{1g}/d_{z^2}	−2.11	−2.12	−2.67	−2.66	−2.87	−2.85	−3.44	−3.40
	$2e_g$	−1.46	−1.40	−1.95	−1.87	−2.27	−2.18	−2.80	−2.69

[a] $R_{Co-N(eq)}$: equatorial Co−N(eq) bond length. E_{bind}: binding energy between Co and $TPPF_x$. IP: ionization potential. EA: electron affinity. [b] See Figure 2 for the orbitals; the first IP is indicated in bold.

Now, from L = Py/Im to L = CO, the relative energies of the high-spin state greatly increase, so that $CoTPPF_{28}(CO)_2$ no longer has a high-spin ground state. The energy ordering between ^4E_g and $^4A_{2g}$ is also reversed in $CoTPPF_{28}(CO)_2$. On the basis of the τ-HCTH results, the lower-lying quartet $^4A_{2g}$ lies ∼0.3 eV above the ground state.

As illustrated in Figure 3, the replacement of the Py ligands by the CO ones lowers all of the MOs. The d_{xy} orbital is particularly stabilized, which may be attributed to metal → CO π^* back-bonding. As a strong-field ligand, CO raises the d_{z^2} orbital energy considerably. Therefore, the a_{1g} (d_{z^2}) orbital in $CoTPPF_{28}(CO)_2$ is much less stabilized than the other d orbitals, and we see a large gap between d_{z^2} and the next occupied d_π orbital.

3.3. Structural and Other Energetic Properties. Table 7 presents the calculated properties (Co−N bond lengths R, $CoTPPF_x$ binding energies E_{bind}, ionization potentials IP, and electron affinities EA) for the unligated $CoTPPF_x$ complexes in their ground state ($^2A_{1g}$), obtained with the VWN-B-P and τ-HCTH functionals. (The τ-HCTH functional does not have an implementation for the potential, but only for the energy.) E_{bind} is defined as the energy required to pull the metal apart from the porphyrin ring

$$-E_{bind} = E(CoTPPF_x) - [E(Co) + E(TPPF_x)]$$

where $E(CoTPPF_x)$, $E(Co)$, and $E(TPPF_x)$ are the total energies of the indicated species. (The geometries of $CoTPPF_x$ and $TPPF_x$ are independently optimized.)

In Table 7, the equatorial Co−N bond lengths ($R_{Co-N(eq)}$) in CoTPP and $CoTPPF_{20}$ are similar (1.97 Å), slightly shorter than in $CoTPPF_8$ and $CoTPPF_{28}$ (1.99 Å). The calculated values and their trend are in good agreement with the X-ray crystal structure data on CoTPP (1.95 Å) and $CoTPPF_{28}(toluene)_2$ (1.99 Å). The calculated E_{bind} is sensitive to the density functional used. The VWN-B-P value is systematically larger than the τ-HCTH value by about 1.1 eV. We believe that τ-HCTH offers higher energetic accuracy than VWN-B-P. Nevertheless, the trend in the results remains unchanged. From CoTPP to $CoTPPF_8$, the E_{bind} decreases by 0.45 eV, indicating that the β-fluorination weakens the interaction between the metal and the ring. The substituents at the *meso*-phenyl positions have an opposite effect, strengthening the interaction.

There are, however, no notable changes in the calculated IPs and EAs from VWN-B-P to τ-HCTH, which may imply error cancellations in the calculations on these properties. According to the results, the first ionization occurs from the porphyrin π-orbital for CoTPP and $CoTPPF_{20}$, while it takes place from a metal 3d orbital for $CoTPPF_8$ and $CoTPPF_{28}$. The calculated IP of ∼6.5 eV for CoTPP is in quantitative agreement with the gas-phase potential energy surface (PES) data (∼6.5 eV).[37] Corresponding to the downshift of the valence MOs (as shown in Figure 2), the IPs increase on going from CoTPP to $CoTPPF_8$ to $CoTPPF_{20}$ to $CoTPPF_{28}$. This pattern is repeated for the calculated EAs. Thus, the introduction of halogen substituents at the periphery of the porphyrin ring can exert a substantial influence on the redox properties of MPors; they increase the oxidation potentials and facilitate reduction reactions. For every $[CoTPPF_x]^-$ (the reduction of $CoTPPF_x$), the added electron occupies the low-lying a_{1g} (d_{z^2}) orbital. With increasing x, there is very slight increase in Q_{Co}.

Table 8 displays the calculated properties for the ligated $CoTPPF_x(L)_2$ complexes. For $CoTPPF_8(Im)_2$ and $CoTPPF_{28}(L)_2$, the results of both low-spin and high-spin states are reported. The binding energy (E_{bind}) in this table now refers to the energy required to pull both L molecules off the complex, namely

$$-E_{bind} = E[CoTPPF_x(L)_2] - [E(CoTPPF_x) + 2E(L)]$$

The VWN-B-P and τ-HCTH calculated E_{bind} values are different by nearly a constant; the difference is 0.1−0.2 eV for the low-spin complexes and 0.5−0.6 eV for the high-spin complexes. Again, no notable changes in the IPs and EAs are found from VWN-B-P to τ-HCTH.

The equatorial Co−N(eq) bond length in the ligated systems shows a very slight core expansion (<0.02 Å) as compared to that in unligated $CoTPPF_x$, indicating that the axial ligands have little stretching effect upon the Co−N(eq) bond length. Owing to the occupation of the $3d_{z^2}$ orbital, the axial Co−L(ax) bond length is relatively large and depends on the spin state. For example, $R_{Co-O(ax)}$ is 2.38 Å in low-spin $CoTPPF_{28}(THF)_2$, but shorter by 0.05 Å when this complex is high-spin. However, there is no notable change of $R_{Co-L(ax)}$ on going from x = 0 to x = 28. On the other hand, the same Co−N(ax) bond is longer in $CoTPPF_x(Py)_2$ than in $CoTPPF_x(Im)_2$ (by ∼0.04 Å). With one electron in the b_{1g} ($d_{x^2-y^2}$) orbital in the high-spin state complexes, the repulsive interaction between the $d_{x^2-y^2}$ electron and those on the pyrrole nitrogens expands the Co−N(eq) bond, by ∼0.06 Å. X-ray crystal structure data on ligated cobalt porphyrins are available only for $CoTPPF_{28}(THF)_2$. While there is very good agreement between the calculated and experimental Co−N(eq) bond lengths (see Table 4), a large difference in $R_{Co-O(ax)}$ is found between the calculation (2.332 Å) and experiment (2.204 Å). Since the Co−THF bond is weak, it may be sensitive to environment: The crystal field stabilization of the molecule may cause a bond length contraction for Co−THF.

The binding energy (E_{bind}) between CoTPP and a pair of THF molecules is small, about 0.1 eV. This quantity grows to ∼0.5 eV for $CoTPPF_{28}$, so the F substituents enhance the axial ligation. Py binds more strongly than does THF, as shown by

TABLE 8: Calculated Properties[a] for Ligated $CoTPPF_x(L)_2$ Complexes (x = 0, 8, 20, 28; L = THF, Py, Im) with the VWN-B-P and τ-HCTH Functionals

		$R_{Co-N(eq)}$ (Å)	$R_{Co-L(ax)}$ (Å)	E_{bind} (eV)	IP[b] (eV)				EA[b] (eV)
Low Spin, $^2A_{1g}$									
					a_{1g}/d_{z^2}	$1b_{3g}/d_{yz}$	$1b_{2g}/d_{xz}$	b_{1u}	$2b_{2g}$
$CoTPP(THF)_2$	VWN−B−P	1.980	2.395	0.14	6.54	**5.86**	5.95	6.15	−1.25
	τ-HCTH			0.08	6.78	**5.79**	5.88	6.12	−1.21
$CoTPPF_8(THF)_2$	VWN−B−P	1.995	2.385	0.27	7.06	**6.31**	6.39	6.72	−1.71
	τ-HCTH			0.19	7.29	**6.23**	6.29	6.68	−1.64
$CoTPPF_{20}(THF)_2$	VWN−B−P	1.980	2.386	0.35	7.12	**6.52**	6.66	7.03	−2.02
	τ-HCTH			0.31	7.35	**6.45**	6.57	6.98	−1.95
$CoTPPF_{28}(THF)_2$	VWN−B−P	1.998	2.376	0.53	7.64	**6.99**	7.11	7.61	−2.52
	τ-HCTH			0.48	7.86	**6.90**	6.99	7.52	−2.43
$CoTPP(Py)_2$	VWN−B−P	1.986	2.307	0.53	**5.34**	5.74	5.74	6.02	−1.27
	τ-HCTH			0.37	**5.53**	5.65	5.65	5.99	−1.22
$CoTPPF_8(Py)_2$	VWN−B−P	2.000	2.308	0.70	**5.88**	6.20	6.20	6.61	−1.72
	τ-HCTH			0.52	**6.07**	6.09	6.09	6.57	−1.66
$CoTPPF_{20}(Py)_2$	VWN−B−P	1.986	2.312	0.79	**5.91**	6.42	6.41	6.86	−2.02
	τ-HCTH			0.63	**6.09**	6.31	6.30	6.82	−1.96
$CoTPPF_{28}(Py)_2$	VWN−B−P	2.001	2.302	1.00	**6.40**	6.87	6.86	7.44	−2.64
	τ-HCTH			0.84	**6.57**	6.74	6.73	7.37	−2.40
Low Spin, $^2A_1$									
					a_1/d_{z^2}	a_2/d_{xz}	$1b_1/d_{yz}$	b_1/b_{1u}	$2b_1$
$CoTPP(Im)_2$	VWN−B−P	1.988	2.265	0.44	**5.19**	5.56	5.58	5.73	−1.09
	τ-HCTH			0.34	**5.42**	5.48	5.49	5.50	−1.05
$CoTPPF_8(Im)_2$	VWN−B−P	2.000	2.273	0.64	**5.79**	6.03	6.05	6.34	−1.55
	τ-HCTH			0.50	6.01	**5.93**	5.94	6.18	−1.48
$CoTPPF_{20}(Im)_2$	VWN−B−P	1.989	2.277	0.80	**5.82**	6.26	6.29	6.49	−1.85
	τ-HCTH			0.70	**6.04**	6.16	6.18	6.26	−1.79
$CoTPPF_{28}(Im)_2$	VWN−B−P	2.011	2.264	1.04	**6.37**	6.75	6.77	7.05	−2.45
	τ-HCTH			0.96	**6.58**	6.63	6.65	6.92	−2.24
High Spin, $^4B_{3g}$									
					$b_{1g}/d_{x^2-y^2}$	a_{1g}/d_{z^2}	$1b_{3g}/d_{yz}$	b_{1u}	$1b_{2g}/d_{xz}$
$CoTPPF_{28}(THF)_2$	VWN−B−P	2.057	2.332	−0.03	**6.55**	8.13	7.13	7.50	−3.03
	τ-HCTH			0.56	6.99	8.66	**6.98**	7.42	−2.96
$CoTPPF_{28}(Py)_2$	VWN−B−P	2.060	2.281	0.39	**6.38**	7.13	6.82	7.35	−3.09
	τ-HCTH			0.89	6.80	7.55	**6.67**	7.28	−2.99
High Spin, $^4B_1$									
					$b_2/d_{x^2-y^2}$	a_1/d_{z^2}	b_1/d_{yz}	b_1/b_{1u}	a_2/d_{xz}
$CoTPPF_8(Im)_2$	VWN−B−P	2.064	2.218	0.05	**5.55**	6.42	6.05	6.09	−2.16
	τ-HCTH			0.52	5.98	6.92	**5.90**	6.17	−2.09
$CoTPPF_{28}(Im)_2$	VWN−B−P	2.073	2.199	0.55	**6.30**	6.97	6.72	6.87	−2.94
	τ-HCTH			1.08	6.73	7.45	**6.56**	6.73	−2.84

[a] $R_{Co-N(eq)}$: equatorial Co−N bond length. $R_{Co-L(ax)}$: axial Co-L bond length. E_{bind}: bind energy between $CoTPPF_x$ and 2L (see text). IP: ionization potential. EA: electron affinity. [b] See Figure 3 for the orbitals; the first IP is indicated in bold.

the larger E_{bind} in Table 8. The binding property of Im is comparable to that of Py.

The first ionizations of $CoTPPF_x(L)_2$ now all occur from a metal d orbital for the various x values. But the d orbital that corresponds to the first IP is different for different L and also depends on the spin state. For L = THF, the weak-field ligand leads to a relatively small rise in d_{z^2}, and so, the electron is first removed from a d_π orbital in low-spin $CoTPPF_x(THF)_2$. With L = Py or Im, however, the first IP of low-spin $CoTPPF_x(L)_2$ corresponds to the removal of an electron from the d_{z^2} orbital. In the case of the high-spin state complexes, the VWN-B-P results show that the first electron is removed from the high-lying $d_{x^2-y^2}$ orbital, but the τ-HCTH results indicate that the low-lying d_{yz} (d_π) orbital is ionized first. Experimental PES measurements may be required in order to determine which d orbital is the first IP orbital.

Owing to the upshift of the MOs, the IPs of $CoTPPF_x(L)_2$ decrease notably as compared to those of $CoTPPF_x$, suggesting that the former will be easier to oxidize than the latter. The axial ligands also decrease the electron affinity, especially for the low spin state complexes, where the added electron occupies the high-lying antibonding porphyrin $2e_g$ (π^*) orbital. For the high spin state complexes, the added electron still goes into a low-lying metal d orbital (now d_{xz}).

4. Conclusions

According to experimental results,[5] there is partial population of the ^4E_g high-spin state in $CoTPPF_{28}(THF)_2$ and $CoTPPF_{28}(Py)_2$ and a complete conversion to the high-spin state in $CoTPPF_{28}(1\text{-MeIm})_2$. All the pure GGA functionals, including the recently developed mPBE, OPBE, and HCTH/407, more or less overestimate the relative energies of the high-spin states. Agreement with the experimental observation is obtained with the meta-GGA functional τ-HCTH, which contains the kinetic energy density (τ). τ-HCTH appears to offer the same energetic accuracy as the hybrid B3LYP functional, which suggests that the "local" τ-form in the meta-GGA is a promising alternative to the "delocalized" exact HF exchange.

It should be pointed out that, although τ-HCTH has provided an adequate description for the electronic structure of the high-spin $CoTPPF_{28}(L)_2$ complexes, we are not sure whether this functional is able to achieve the same accuracy for other difficult, transition-metal systems. An extensive test of a large number of density functional formalisms on iron porphyrins and related compounds is in progress, and the results will be published in a separate paper. In fact, so far, no one has found a universally "best" functional for accurate prediction of geometries and energies of varieties of systems. To obtain accurate results, there is a need to test the performance of different functionals.

F substituents at the β-pyrrole position of the porphyrin cause a decrease of ~0.15 eV in the relative energies (E^{relative}) of the high-spin states. However, the fluorination at the *meso*-phenyl periphery has little influence on the E^{relative}. For many properties, CoTPP is similar to $CoTPPF_{20}$ and $CoTPPF_8$ is similar to $CoTPPF_{28}$. Upon coordination by two weak or intermediately strong field axial ligands such as THF, Py, or Im, the E^{relative} further decreases by ~0.5 eV, and so, the energy order between the low-spin and high-spin states in $CoTPPF_{28}$ is reversed. The τ-HCTH calculated E^{relative} values and their trend are in agreement with the experimental results.[5] The calculations on $CoTPPF_8(L)_2$ (L = THF, Py, Im) suggest the low-spin and the high-spin states to be nearly degenerate in energy. When two strong-field axial CO ligands coordinate, every $CoTPPF_x(CO)_2$ complex becomes low-spin, having a $^2A_{1g}$ ground state, like unligated $CoTPPF_x$.

Corresponding to the downshifts of the valence MOs caused by the peripheral substituents, both ionization potential (IP) and electron affinity (EA) increase from CoTPP to $CoTPPF_8$ to $CoTPPF_{20}$ to $CoTPPF_{28}$. The results account for the fact that halogenated porphyrins are more difficult to oxidize but easier to reduce than unsubstituted porphyrins. Substitution by the F atoms also significantly increases the binding strength between the metal porphyrin and the axial ligands. As an axial ligand with strong σ-donor but weak π back-bonding ability, L raises the MO energy levels; both the IP and EA of $CoTPPF_x(L)_2$ are decreased relative to those of $CoTPPF_x$. Thus, axial ligation also has a substantial influence on the redox properties of metal porphyrins.

Acknowledgment. This work was supported by the National Institutes of Health (S06 GM08047).

Supporting Information Available: Comparison of the calculated properties of the $CoTPPF_x$ (x = 0, 8, 20, 28) optimized D_{2d} and D_{4h} structures (Table S1). Comparison of the relative energies for selected states of CoTPP obtained with the frozen-core approximation and all-electron calculations (Table S2). Comparison of the calculated properties between the free molecule and the molecule in dichloromethane solvent (Table S3). Calculated relative energies for selected states of $CoTPPF_x(L)_2$ (x = 0, 8, 20, 28; L = Py, Im, CO) with various density functionals (Tables S4−S6). This material is available free of charge via the Internet at http://pubs.acs.org.

References and Notes

(1) (a) Mashiko, T.; Dolphin, D. In *Comprehensive Coordination Chemistry*; Wilkinson, G., Ed.; Pergamon: Oxford, 1987; Vol. 2. (b) Latos-Grazynski, L.; Rachlewicz, K.; Wojaczynski, J. *Coord. Chem. Rev.* **1999**, *190*−*192*, 109. (c) Meunier, B. *Chem. Rev.* **1992**, *92*, 1411. (d) Dolphin, D.; Traylor, T. G.; Xie, L. Y. *Acc. Chem. Res.* **1997**, *30*, 251. (e) Smith, K. M. In *Comprehensive Heterocyclic Chemistry*; Katritzky, A. R., Rees, C. W., Eds.; Pergamon: Oxford, 1984; Vol. 4.

(2) (a) Kadish, K. M.; D'Souza, F.; Villard, A.; Autret, M.; van Caemelbecke, E.; Bianco, P.; Antonini, A.; Tagliatesta, P. *Inorg. Chem.* **1994**, *33*, 5169. (b) Spyroulia, G. A.; Despotopoulos, A. P.; Raptopoulou, C. P.; Terzis, A.; de Montauzon, D.; Poilblanc, R.; Coutsolelos, A. G. *Inorg. Chem.* **2002**, *41*, 2648.

(3) Chen, H. L.; Ellis, P. E.; Wijesekera, T.; Hagan, T. E.; Groh, S. E.; Lyons, J. E.; Ridge, D. P. *J. Am. Chem. Soc.* **1994**, *116*, 1086.

(4) Woller, E. K.; DiMagno, S. G. *J. Org. Chem.* **1997**, *62*, 1588.

(5) Smirnov, V. V.; Woller, E. K.; DiMagno, S. G. *Inorg. Chem.* **1998**, *37*, 4971.

(6) Lai, S.-W.; Hou, Y.-J.; Che, C.-M.; Pang, H.-L.; Wong, K.-Y.; Chang, C. K.; Zhu, N. *Inorg. Chem.* **2004**, *43*, 3724.

(7) Liao, M.-S.; Scheiner, S. *J. Chem. Phys.* **2002**, *116*, 3635.

(8) Nguyen, K. A.; Day, P. N.; Pachter, R.; Tretiak, S.; Chernyak, V.; Mukamel, S. *J. Chem. Phys.* **2002**, *106*, 10285.

(9) Ghosh, A. *Acc. Chem. Res.* **1998**, *31*, 189.

(10) Becke, A. D. *J. Chem. Phys.* **1993**, *98*, 5648.

(11) van Voorhis, T.; Scuseria, G. E. *J. Chem. Phys.* **1998**, *109*, 400.

(12) Proynov, E.; Chermette, H.; Salahub, D. R. *J. Chem. Phys.* **2000**, *113*, 10013.

(13) Boese, A. D.; Handy, N. C. *J. Chem. Phys.* **2002**, *116*, 9559.

(14) Perdew, J. P.; Burke, K.; Ernzerhof, M. *Phys. Rev. Lett.* **1996**, *77*, 3865.

(15) Zhang, Y.-K.; Yang, W.-T. *Phys. Rev. Lett.* **1998**, *80*, 890.

(16) Hammer, B.; Hansen, L. B.; Nørskov, J. K. *Phys. Rev. B* **1999**, *59*, 7413.

(17) Adamo, C.; Barone, V. *J. Chem. Phys.* **2002**, *116*, 5933.

(18) Hamprecht, F. A.; Cohen, A. J.; Tozer, D. J.; Handy, N. C. *J. Chem. Phys.* **1998**, *109*, 6264.

(19) Boese, A. D.; Handy, N. C. *J. Chem. Phys.* **2001**, *114*, 5497.

(20) Ghosh, A.; Vangberg, T.; Gonzalez, E.; Taylor, P. *J. Porphyrins Phthalocyanines* **2001**, *5*, 345.

(21) Truong, T. N.; Stefanovich, E. V. *J. Phys. Chem.* **1995**, *99*, 14700.

(22) Madura, P.; Scheidt, W. R. *Inorg. Chem.* **1976**, *15*, 3182.

(23) (a) Liao, M.-S.; Scheiner, S. *J. Chem. Phys.* **2002**, *117*, 205. (b) Piet, D. P.; Danovich, D.; Zuilhof, H.; Sudhölter, E. J. R. *J. Chem. Soc., Perkin Trans. 2* **1999**, 1653.

(24) Baerends, E. J.; Ellis, D. E.; Roos, P. *Chem. Phys.* **1973**, *2*, 41.

(25) te Velde, G.; Bickelhaupt, F. M.; van Gisbergen, S. J. A.; Fonseca-Guerra, C.; Baerends,E. J.; Snijders, J. G.; Ziegler, T. *J. Comput. Chem.* **2001**, *22*, 931.

(26) Fonseca-Guerra, C.; Snijders, J. G.; Baerends, E. J.; te Velde, G. *Theor. Chem. Acc.* **1998**, *99*, 391.

(27) *ADF2004.01*; SCM: Theoretical Chemistry, Vrije Universiteit, Amsterdam, The Netherlands; http://www.scm.com.

(28) Vosko, S. H.; Wilk, L.; Nusair, M. *Can. J. Phys.* **1980**, *58*, 1200.

(29) Becke, A. D. *Phys. Rev. A* **1988**, *38*, 3098.

(30) Perdew, J. P. *Phys. Rev. B* **1986**, *33*, 8822.

(31) Adamo, C.; Barone, V. *J. Chem. Phys.* **1998**, *108*, 664.

(32) Handy, N. C.; Cohen, A. J. *Mol. Phys.* **2001**, *99*, 403.

(33) Lee, C.; Yang, W.-T.; Parr, R. G. *Phys. Rev. B* **1988**, *37*, 785.

(34) Ziegler, T.; Tschinke, V.; Baerends, E. J.; Snijders, J. G.; Ravenek, W. *J. Phys. Chem.* **1989**, *93*, 3050.

(35) Lin, W. C. *Inorg. Chem.* **1976**, *15*, 1114.

(36) We find that the B3LYP calculated relative energies of ^2E_g and ^4E_g (which are 1.07 and 1.68 eV, respectively, for CoTPP) are unreasonable. It is stated that, for the present version of ADF, hybrid functionals cannot be used in combination with frozen cores (ADF2004.01 User's Guide).

(37) Khandelwal, S. C.; Roebber, J. L. *Chem. Phys. Lett.* **1975**, *34*, 355.